The Effects of Mixture Preburning on Detonation Wave Propagation

Supraj Prakash[a,*], Venkat Raman[a]

[a]*Department of Aerospace Engineering, University of Michigan, Ann Arbor, MI 48109, USA*

Abstract

Pressure gain combustion in the form of continuous detonations can provide a significant increase in the efficiency of a variety of propulsion and energy conversion devices. In this regard, rotating detonation engines (RDEs) that utilize an azimuthally-moving detonation wave in annular systems are increasingly seen as a viable practical approach to realizing pressure gain combustion. However, practical RDEs that employ non-premixed fuel and oxidizer injection need to minimize losses through a number of mechanisms, including turbulence-induced shock-front variations, incomplete fuel-air mixing, and premature deflagration. In this study, a canonical stratified detonation configuration is used to understand the impact of preburning on detonation efficiency. It was found that heat release ahead of the detonation wave leads to weaker shock fronts, delayed combustion of partially-oxidized fuel-air mixture, and non-compact heat release. Furthermore, large variations in wave speeds were observed, which is consistent with wave behavior in full-scale RDEs. Peak pressures in the compression region or near triple points were considerably lower than theoretically-predicted values for ideal detonations. Analysis of the detonation structure indicates that this deflagration process is parasitic in nature, reducing the detonation efficiency but also leading to heat release far behind the wave that cannot directly strengthen the shock wave. This parasitic combustion leads to commensal combustion (heat release far downstream of the wave), indicating that it is the root cause of combustion efficiency losses.

Keywords:
Rotating detonation engine, Parasitic combustion, Stratification, Direct numerical simulation

*Corresponding author: Supraj Prakash
Email address: suprajp@umich.edu (Supraj Prakash)

1. Introduction

Rotating detonation engines (RDEs) are a feasible approach to realizing pressure gain combustion. However, practical implementation of these devices requires the use of non-premixed discrete fuel-oxidizer injection [1, 2]. Many different injector designs have been considered, including the radial configuration [2], impinging jets [3, 4], and axial systems [5, 6]. Regardless of the design, the aerodynamically-driven turbulent mixing is always imperfect, leading to a stratified fuel-air mixture that is processed by the detonation wave. In practical systems, this variability in the level of mixing can critically affect the detonation wave. For instance, typical wave velocities are considerably lower than the Chapman-Jouguet (CJ) speed [1, 2, 7], which is partially caused by reduced heat release behind the shock wave. While different mechanisms for this reduction have been postulated [5, 8, 9], one main cause is so-called parasitic combustion [5, 10, 11]. In this regime, in addition to incomplete mixing, interaction with product gases from the previous cycle can lead to premature deflagration and heat release. For instance, Chacon et al. [12] found two distinct regions of deflagration: 1) recirculation of product gases trapped near the inlet due to injector design, and 2) a contact burning region caused by mixing between product gases and incoming fresh gases (preburning effect). The former flameholding feature is not universal, but depends on the injector configuration used [13]. The latter preburning mechanism is the focus of the present study.

Numerical studies of full-scale RDE systems have suggested that up to 35-50% preburning of the fuel-oxidizer mixture is prevalent within the combustor [11, 14]. Detonation waves in RDEs are structurally different from ideal premixed waves [15]. Due to incomplete mixing, flow property variations can lead to a weaker shock wave, which in turn lengthens the induction zone. A delayed heat release profile moves the thermal choke further behind the wave front, leading to reduced wave speeds. In discrete injection systems, such wave structure may occupy the entire inter-injector distance [9] with multiple compression-expansion waves present in the induction zone. If deflagrated products are present ahead of the wave, this further weakens the shock and may even cause the reaction layer to detach. For instance, Fig. 1 shows an instantaneous image from a full system calculation for a hydrogen-air system [16]. Here, it is seen that although the detonation wave is followed by a temperature change, there are regions ahead of the wave (especially near the bottom of the domain) where temperature is rising despite not yet being processed by the shock wave. In practical RDEs, this weakening results in higher fraction of heat release in the deflagration mode (lower pressure, volumetrically distributed) rather than the detonation mode (higher pressure, compact region). Since detonation combustors are not optimized for deflagrative heat release, even with complete fuel consumption, the net efficiency may become lower than conventional deflagrative combustors.

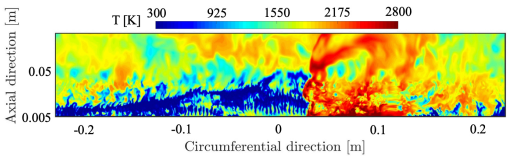

Figure 1: Snapshot of temperature profile from a three-dimensional full-system simulation shown as an unwrapped image at the mid-channel location. Reproduced from [16].

In the past, numerical and experimental studies have been conducted to understand the impact of stratification on detonation propagation [17–20]. The mixture inhomogeneity results in a skewed detonation wave front, with irregular detonation cell structures [17] and diminished wave propagation velocities [20]. Spatial inhomogeneity has been previously studied through one- and two-dimensional numerical simulations with single-step Arrhenius chemical kinetics by introducing a detonation wave to discrete reactive layers and squares, respectively [21]. With sufficiently inhomogeneous mixtures, where the spacing between successive reactive zones is greater than the reaction zone length, a "super-CJ" wave behavior is observed, with propagation speeds 15% higher than the CJ speed of a homogeneous mixture [22]. Discretely placed fuel sources thus act as concentrated pockets of energy release, and enforce a nonequilibrium state for the detonation wave.

With this background, the focus of this study is to isolate the effect of preburning on detonation propagation. For this purpose, a canonical flow configuration with quiescent initial flow but stratification of fuel-air mixture is considered. Based on prior work that considers only the role of stratification [23], the current work introduces the effect of preburning by imposing deflagration ahead of the wave. Detailed multi-step kinetics are used to study the evolution of the shock-driven combustion process. Specific operating parameters are obtained from full-scale RDE calculations [11, 16].

2. Simulation configuration and numerical approach

To replicate the wave structure in a practical RDE geometry, a canonical channel geometry of length 14 cm, width 7.6 mm, and height 6.25 cm is modeled as shown

in Fig. 2. The height of the channel corresponds to the characteristic large length scale, L_{char}, within the domain. As an extension of past studies of Prakash et al. [15], the operating pressure of half the atmospheric condition with background air is used. The channel is confined with walls in the stream normal and spanwise direction, and the right boundary is set as an outflow. The inflow boundary condition is prescribed by a sampled right-running, well-developed, three-dimensional detonation wave. The grid for the three-dimensional geometry consists of 1) a uniform resolution core region and 2) a near-wall region. A near-wall region in the stream normal and spanwise directions contain clustered cells to properly resolve the boundary layer. Note that the near-wall regions are not included in the analysis, but the higher resolution is maintained to ensure that non-physical flow is not developed. This results in a total of 303 million cells, with $2800 \times 858 \times 126$ points in the x, y and z directions, respectively. Within the uniform core region, $\Delta y = \Delta z = 75$ μm, and $\Delta x = 50$ μm. The near-wall region is characterized by $\Delta y = \Delta z = 3.2$-$74.7$ μm. The clustered grid near the wall extends up to 435 y^+, or 0.261 mm, from the wall, where one y^+ is 0.6 μm. The length scale of interest is the induction length ℓ, which, for stoichiometric hydrogen-air detonation at these operating conditions, is analytically given by 398 μm. Thus, approximately 6-8 grid points are used to resolve the induction length.

The range of equivalence ratios is set to be between 0.75 and 1.5, which is based on full-system RDE calculations [11]. Fuel-air stratification is introduced in the form of patches of varying equivalence ratios sampled from a model energy spectrum as per the methods of Ref. [24, 25]. An integral length scale is used as an input to create a corresponding homogeneous isotropic distribution with no mean gradient present. In this sense, this study is different from prior detonation studies with concentration gradients [20, 26]. In the selection of conditions for this study, a study of a full-scale hydrogen-air RDE with axial air inlet is utilized [16]. An integral length scale of 4.3 mm, extracted from the full-scale RDE data, is applied to the scalar energy spectrum function. Note that this length scale is roughly 10 times the induction length of an ideal detonation under these conditions. The resulting fuel-air distribution in terms of equivalence ratio is shown in Fig. 2.

From the three-dimensional RDE data, a one-dimensional profile along an azimuthal path at the mid-channel location and 2 cm height from the injectors is obtained. The profile is temporally-averaged about the wave front location. Data was collected at a height identified from mixing analysis performed by Sato et al. [16] as a location strongly affected by parasitic combustion due to recirculation zones and injector dynamics. Thus, the region was characterized by reduced detonation strength due to mixture inhomogeneity and preburning. Figure 3 shows this nominal profile along the azimuthal or circumferential direction. It is seen that the peak in pressure is reached close to $\bar{x} = 0$, which defines the location of the detonation wave. The temperature profile progressively decreases, which indicates that fresh gases at a lower temperature are entering this region. However, at $\bar{x} > 0.7$, temperature begins to increase even though the pressure profile observes either nearly constant or slightly decaying behavior. This is the region of deflagration, where autoignition of pockets of fuel and air mixed with product gases from previous cycle has initiated. The parameters for the current study are extracted from the region $\bar{x} = 0.7 - 1$.

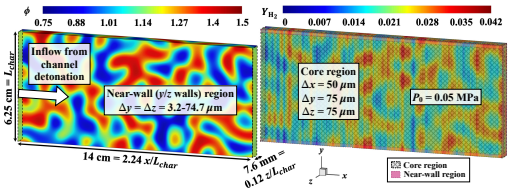

Figure 2: (Left) Contour of local equivalence ratio and (right) H_2 mass fraction along with description of the three-dimensional channel domain for a preburnt mixture with integral length scale of 4.3 mm. The uniform core and near-wall (y/z walls) grid regions are denoted in the right image.

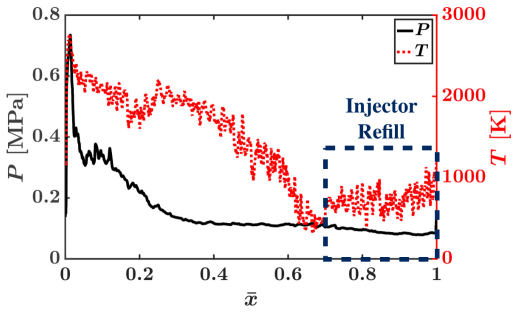

Figure 3: Temporally-averaged (about the wave front location) pressure and temperature profiles from the axial air inlet full-scale RDE simulations unwrapped into a one-dimensional profile as a function of normalized azimuthal distance, reproduced from [16].

To introduce the preburning effect, the following procedure is used. Based on the local equivalence ratio shown in Fig. 2, a corresponding equilibrium solution based on deflagration at constant pressure is obtained. The species composition at each point in the computational domain is then updated towards this equilibrium:

$$Y_{pb}(\boldsymbol{x}, 0) = Y(\boldsymbol{x}, 0) + f\left(Y_{eq}(\boldsymbol{x}) - Y(\boldsymbol{x}, 0)\right), \qquad (1)$$

where Y_{eq} and Y_{pb} denotes the equilibrium and partially-burnt compositions, respectively, corresponding to the initial fuel mass fractions $Y(\boldsymbol{x}, 0)$ at a particular spatial location. Here. f is the preburning ratio, a fractional measure of deflagration.

In order to associate f to the local composition, the preburning ratio is defined using a progress variable $c = Y_{H_2O} + Y_{OH}$. Thus, it follows that f can be defined as a ratio of the local progress variable to its value at equilibrium as:

$$f = \frac{Y_{H_2O} + Y_{OH}}{\left[Y_{H_2O} + Y_{OH}\right]_{eq}} = \frac{c}{c_{eq}} \tag{2}$$

From the full-scale RDE data described in Fig. 3, the distribution of f is shown in Fig.4. It is seen that f has a high degree of linear correlation with the normalized temperature. This linear relation shows that data in this region is dominated by constant pressure deflagration. From the RDE data of a small number of detonation cycles, a short-time averaged profile of f along the direction of wave propagation is obtained. The short time average is used to ensure that significant fluctuations in equivalence ratio is not present, in order to preserve the homogeneous initial conditions. The region from $\bar{x} = 0.7 - 1$ from the full-scale RDE (Fig. 3) represents a length equal to 0.14 cm.

This directional profile of f from $\bar{x} = 0.7-1$ is flipped then imposed in the streamwise direction on the initial condition given in Fig. 2, along with Eq. 1, to obtain the preburning-based initial condition that is also shown in Fig. 2. As a result, the profile of f at $\bar{x} = 1.0$ is applied at the entrance to the channel and the profile at $\bar{x} = 0.7$ location is at the exit of the channel. The preburning ratio varies in the streamwise direction, and is homogeneous in the stream normal directions. Note that the wall confinement and three-dimensionality of the flow is necessary to ensure propagation of triple points along the detonation front. Furthermore, the mixture within the channel geometry is allowed to burn as the detonation wave inflow travels through the domain. Consequently, the mixture near the exit of the channel (with a preburning ratio corresponding to $\bar{x} = 0.7$) continues to burn until the detonation wave arrives at this location in the channel, thereby increasing the local level of burning with time. Because the detonation wave travels at a finite speed similar to the RDE system, time for deflagration is roughly constant at each streamwise location. No diffusion-based flames are established during the burning process as the time-scale of their development will be much longer than the time taken for the shock to pass through the domain.

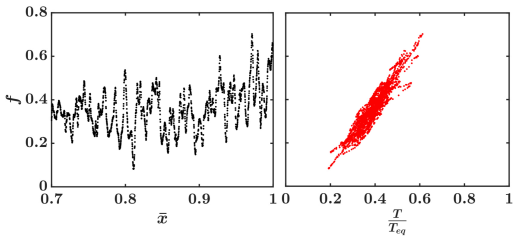

Figure 4: (Left) Preburning ratio f from the injector refill region and (right) correlation of preburning ratio with local temperature to equilibrium temperature for the local composition.

A direct numerical simulation (DNS) approach is applied to study the detonation wave structure in canonical systems. The governing equations of fluid flow consist of mass, momentum, and energy conservation equations supplemented by species conservation equations that incorporate chemical reactions. The system of equations is closed using the ideal gas equation of state.

These governing equations are implemented in an in-house compressible flow solver, UTCOMP. This solver has been extensively validated in the past for a variety of shock-containing flows including scramjet isolators [27, 28], scramjet combustors [29], nonequilibrium flows [30] and detonating flows [15]. The solver utilizes a structured grid configuration with a cell-centered, collocated variable arrangement. A 5^{th} order weighted essentially non-oscillatory (WENO) scheme is used for computing the non-linear convective fluxes [31] and the non-linear scalar terms are calculated using a quadratic upstream interpolation for convective kinematics (QUICK) scheme [32]. A 4^{th} order central scheme is used to calculate the diffusion terms, used to capture the large-scale turbulent structures in the post-detonation region. Explicit time-stepping is performed using a 4^{th} order Runge-Kutta scheme for the temporal discretization. Molecular transport is not included within these simulations as the primary scope of this work is detonaton propagation through an inhomogeneous mixture. The composition and distribution of the inhomogeneous mixture is postulated from RDE data [16] and used as the initial condition.

The solver is parallelized using MPI-based domain decomposition and linear scalability has been demonstrated up to 65,000 cores for similar problems. The detailed chemistry is modeled for hydrogen-oxygen combustion with a nitrogen diluter using a 9-species 19-reaction chemical mechanism derived from Mueller et al. [33] using CHEMKIN-based subroutines [34]. The solver has been previously validated for hydrogen-air and hydrogen-oxygen detonation using one-, two- and three-dimensional canonical cases [15].

In a confined channel of equivalent cross-section filled with a homogeneous stoichiometric hydrogen-air mixture, a fully-developed detonation wave is created and sampled as a three-dimensional time-varying field to be used as the inflow.

3. Results and discussion

3.1. General behavior

As the detonation wave travels through the stratified mixture from left to right, it exhibits a nearly steady behavior shown in Fig. 5. The wave front is marked by a thin shock region with a trailing reaction zone. Behind this reaction layer, the expansion waves originating from the triple points lead to the creation of both vortical structures and a mixing region. The mixing region is sustained over significant length, and is finally dissipated by viscous forces. Ahead of the wave, density variations caused by the imposed f profile is seen manifesting as striations due to the streamwise-only variation of this quantity. Prior studies [23] have shown that the size of these vortices is related to the stratification length scale. Further, the generation of vortices is consistent with the complex shock structure seen in detonation waves passing over discrete injectors [15, 35].

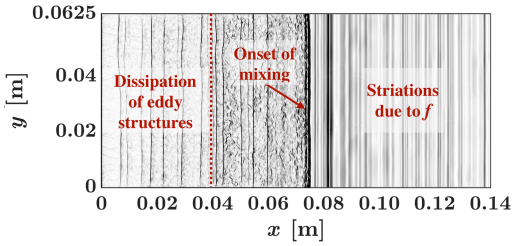

Figure 5: Contour of density gradient at the depth-wise mid-channel plane as the wave is midway through the channel, highlighting the reaction zone and turbulent mixing imposed by the detonation wave.

Figure 6 shows the pressure contour at an intermediate time, with an inset view of the triple points along the wave front. The peak pressure observed is roughly 0.8 MPa, which is less than half the ideal peak pressure of 1.7 MPa for an average equivalence ratio of 1.12 at the ambient conditions of 0.05 MPa and 300 K. More importantly, these peak pressures are observed only at triple points, with much lower values across the detonation front. Note that even after the detonation wave has passed through the region, the pressure variations still persist. This is due to the fact that the wave is traveling at supersonic speeds, while the pressure waves are relaxing at acoustic speed in the post-detonation gases. It is also seen that small amounts of hydrogen remains behind the wave, denoting some reduction in combustion efficiency even for this canonical case. In practical RDEs, this residual fuel-air mixture is found to deflagrate as it convects downstream.

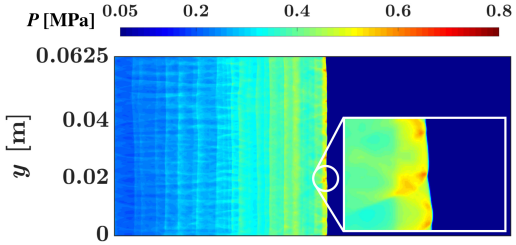

Figure 6: Contour of pressure at the depth-wise mid-channel plane as the wave is midway through the channel. A microscopic view of the triple point structure along the wave front is provided.

A key quantitative measure of shock strength is its propagation velocity. Figure 7 illustrates the variation in wave speed measured locally across the entire simulation. The simulation domain is set up such that the strong homogeneous detonation wave enters from the left and progresses through the stratified mixture. It is seen that the wave velocity exhibits very large fluctuations with variations of up to nearly 500 m/s about the average over short segments of the domain. The instantaneous oscillations in wave velocity are due to changes in local composition and density. This "galloping" feature has been observed in most practical RDEs [1, 12]. The pressure profiles show that the shock front is nearly normal to the propagation direction, and is not as corrugated as seen in practical RDEs [2] given the lack of large scale turbulence found in full scale systems.

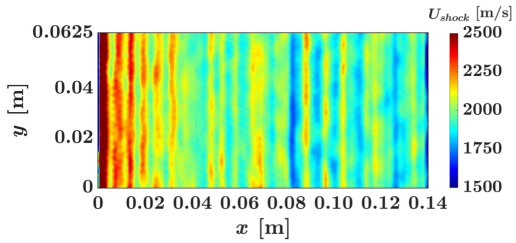

Figure 7: Contour of wave velocity at the depthwise mid-channel plane.

Figure 8 shows the streamnormal-averaged wave velocity as a function of axial position and the PDF of wave velocity within different regions of the domain. As seen in Fig. 7, there is a slow decay in propagation speed with streamwise distance. Regardless, the full computational domain PDF of wave velocity shows a large spread, with the most probable velocity close the CJ speed of 1960 m/s for this operating condition. The PDFs of velocity sampled in 2 cm wide sub-domains within the full domain highlights that the spread of velocities remain approximately unchanged over the different sub-domains at locations downstream. While

there is considerable statistical variation, there is no clear trend in the peak of the PDF moving towards lower velocity values. Thus, the wave velocity exhibits sustained fluctuations but constant wave propagation on an average in the latter part of the domain ($x > 0.08$ m). Note that while stratification can lead to slight increase in speeds due discrete energy source effects as noted by [21], the high observed wave speeds for the available reduced energy may be a consequence of the finite domain length. In other words, a quasi-steady state might not have been reached by the end of the computational domain. However, these results indicate that even in the absence of turbulence-induced wrinkling of detonation front, the wave behavior in this canonical system is similar to that of practical RDEs.

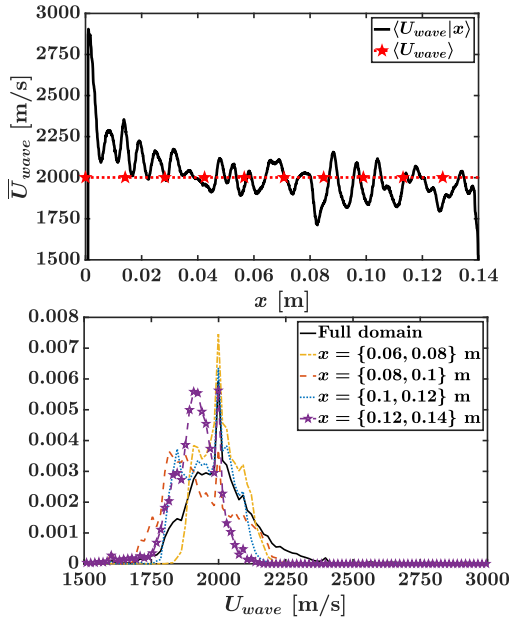

Figure 8: (Top) Wave velocity averaged in stream normal direction and (bottom) PDF of wave velocity within 2 cm sectors of the latter half of the domain compared to the PDF sampled from the entire domain.

3.2. Detonation structure

In order to gain insight into the detonation process across the wave, spatially and temporally-averaged one-dimensional profiles of properties across the wave front are provided in Fig. 9. The wave front location is tracked and a normal vector at every $\{y, z\}$ location on the wave front surface is determined. Thus, the shock front location is assumed to be the same for each surface-normal vector. The one-dimensional profile extracted along this vector at each location across the front surface is then temporally-averaged to obtain a representative one-dimensional profile of properties across the detonation wave. The pressure profile shows interesting features. First, the pressure jump across the wave is much smaller than the theoretical expectation of ~34x (from 0.05 MPa to 1.7 MPa), with an observed pressure jump of only ~8x to 0.5 MPa. The initial shock wave is roughly 200 μm in thickness, which provides compression to raise the fluid temperature by nearly 1000 K. Denoted by position A, the increase in temperature occurs simultaneously with shock compression. However, the subsequent heat release increases the temperature only by 600-700 K, indicating reduced heat release due to preburning. This effect is seen in the heat release plot, with a small positive heat release in the pre-shock region and a large negative heat release in the induction region followed by the combustion process leading to high energy release. Further, the heat release process, highlighted by position B, continues further away from the compression wave, with slow expansion of the gases, with the release rate still higher than the pre-shock preburning values. This delayed heat release is another source of efficiency loss, resulting in so-called commensal combustion or leakage process [12], whereby the energy release does not directly support the wave propagation process.

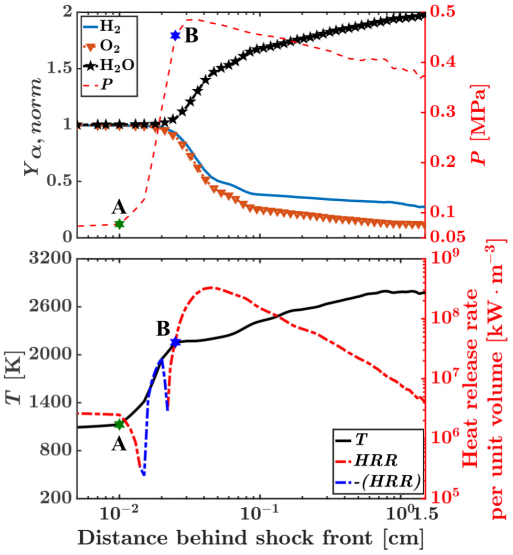

Figure 9: Spatially and temporally averaged one-dimensional profiles of properties across the detonation wave front. Similar positions behind the shock front between both profiles are marked by positions A and B.

The statistical properties of the detonation front show a complex process (Fig. 10). First, it is seen that the normalized pressure and temperature fluctuations peak in the compression region associated with the shock. This indicates that as the wave propagates through the domain, there are large variations in the structure of the

shock wave. This fluctuation is caused by the transverse motion of the triple points (Fig. 6) as well as the variations in the preburning ratio. The fluctuations for hydrogen mass fraction appear downstream of this region, in the post-combustion zone. This variation is merely caused by the changes in post-shock temperature and pressure that leads to reduced consumption of fuel. As seen in the average species mass fraction plot (Fig. 9), hydrogen is depleted near the induction zone, but appreciable fraction is still present far downstream. For comparison, the equilibrium mass fraction at stoichiometric condition for H_2 and 1000 K preburning temperature is approximately 0.0033, while nearly 3 times this mass fraction is found at distances of up to 1 cm behind the wave.

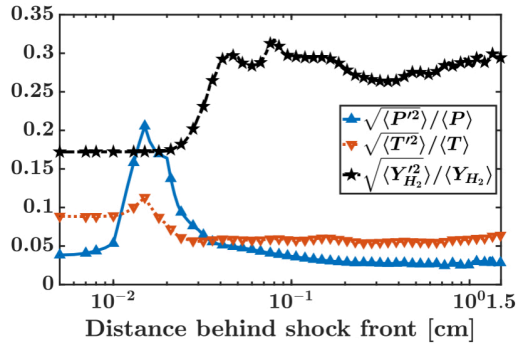

Figure 10: Normalized standard deviation of temperature, pressure, and hydrogen mass fraction across the detonation wave front.

Finally, heat release rate per unit volume conditioned on pressure is shown in Fig. 11. The first notable feature is that high heat release rate is directly associated with higher pressure. Although lower heat release rate is possible at all pressures, the shock-based compression is necessary to increase the compactness of the combustion process. However, the peak heat release does not occur at the highest pressure, which is also seen from Fig. 9. Furthermore, appreciable heat release continues to occur at a distance of 1 cm behind the wave (as noted above).

4. Conclusions

Practical RDEs exhibit combustion inefficiencies due to a number of factors including turbulence-induced wave front wrinkling, incomplete mixing, and premature deflagration or preburning. In this study, the preburning process is isolated by using a canonical system, where a prescribed preburning profile is used. A near-ideal detonation wave formed in a homogeneous and stoichiometric mixture is introduced into the domain with this stratified mixture and fixed preburning profile. Analysis of the wave propagation and detona-

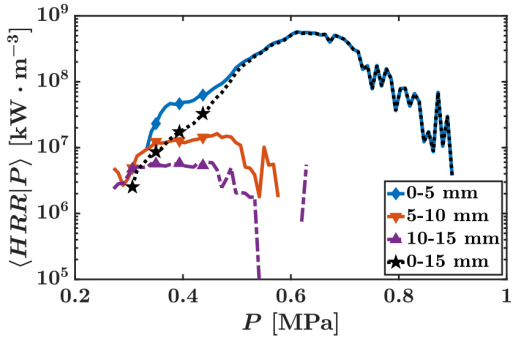

Figure 11: Conditional average of heat release rate per unit volume conditioned on pressure at different distance ranges behind the detonation wave front.

tion structure was conducted.

The detonation wave was found to propagate with a spread of speeds, indicating that the preburning of the mixture significantly affects the strength of the leading shock. The most probable speed was close to the CJ speed, but the standard deviation was ±15%, even for equivalence ratios variations that are small compared to practical RDEs. The detonation wave exhibited a complex structure, with a mixing region behind the propagating front where vortical structures of length scales comparable to the stratification length scale were created. Overall, the detonation structure was weaker, with even the triple points exhibiting lower peak pressures compared to expected theoretical values.

The shock weakening was directly related to the preburning of the fuel-air mixture. The initial compression was smaller than theoretical values, with average pressure increase of approximately 8 times the pre-shock pressure. As a result, the induction zone was much longer, leading to slower heat release extending far behind the shock front, where vortex-driven mixing enforced homogenization of fuel-air mixtures.

These results indicate an important connection between pre-shock deflagration and loss of efficiency. In general, to have a compact heat release zone, it is necessary to have a strong compression wave. Any reduction in peak pressure can adversely affect the heat release profile. The premature deflagration process directly weakens this shock front, leading to a slow and distributed heat release. There is considerable unburnt fuel downstream of the shock front. In other words, so-called parasitic combustion (deflagration ahead of wave) directly leads to commensal combustion (heat release far downstream of the wave), indicating that parasitic combustion is the root cause of loss of combustion efficiency. The fact that these features could be reproduced without significant turbulence in the system indi-

cates that turbulence is more critical to the fuel-air mixing ahead of the shock rather than shock propagation itself.

Acknowledgments

The research is based on work supported the NASA ARMD Fellowship under grant No. 80NSSC18K1735 with Dr. Tomasz Drozda as technical adviser and US DOE/NETL UTSR under grant Nos. DE-FE0025315 and DE-FE0023983 with Mark Freeman and Robin Ames as the technical monitors, respectively. The authors are grateful for NASA HECC computational resources. The authors thank Mr. Takuma Sato for the full-system RDE simulation data used in this study.

References

[1] K. Schadow, E. Gutmark, Combustion instability related to vortex shedding in dump combustors and their passive control, *Prog. in Energy and Combust. Sci.* 18 (1992) 117 – 132.

[2] B. A. Rankin, *et al.*, Chemiluminescence imaging of an optically accessible non-premixed rotating detonation engine, *Combustion and Flame* 176 (2017) 12–22.

[3] F. A. Bykovskii, S. A. Zhdan, E. F. Vedernikov, Continuous spin detonation of hydrogen-oxygen mixtures. 1. annular cylindrical combustors, *Combust., Expl., and Shock Waves* 44 (2008) 150–162.

[4] A. Kawasaki, *et al.*, Critical condition of inner cylinder radius for sustaining rotating detonation waves in rotating detonation engine thruster, *Proc. Combust. Inst.* 37 (2019) 3461–3469.

[5] F. Chacon, M. Gamba, Study of parasitic combustion in an optically accessible continuous wave rotating detonation engine, AIAA Paper, 2019-0473, 2019.

[6] J. Kindracki, P. Wolański, Z. Gut, Experimental research on the rotating detonation in gaseous fuels–oxygen mixtures, *Shock waves* 21 (2011) 75–84.

[7] J. Wilhite, *et al.*, Investigation of a rotating detonation engine using ethylene-air mixtures, AIAA Paper 2016-1650, 2016.

[8] D. P. Stechmann, S. D. Heister, A. J. Harroun, Rotating detonation engine performance model for rocket applications, *Journal of Spacecraft and Rockets* 56 (2018) 887–898.

[9] J. R. Burr, K. Yu, Characterization of CH4-O2 detonation in unwrapped RDE channel combustor, AIAA Paper 2019-4215, 2019.

[10] D. E. Paxson, Examination of wave speed in rotating detonation engines using simplified computational fluid dynamics, AIAA Paper 2018-1883, 2018.

[11] T. Sato, S. Voelkel, V. Raman, Detailed chemical kinetics based simulation of detonation-containing flows, ASME Paper GT2018-75878, 2018.

[12] F. Chacon, M. Gamba, OH PLIF visualization of an optically accessible rotating detonation combustor, AIAA Paper, 2019-4217, 2019.

[13] S. Prakash, *et al.*, Numerical Simulation of a methane-oxygen rotating detonation rocket engine, Submitted to Proc. Combust. Int., 2020.

[14] P. A. Cocks, A. T. Holley, B. A. Rankin, High Fidelity Simulations of a Non-premixed Rotating Detonation Engine, AIAA Paper 2016-0125, 2016.

[15] S. Prakash, *et al.*, Analysis of the detonation wave structure in a linearized rotating detonation engine, *AIAA J.* (2019) 1–15.

[16] T. Sato, *et al.*, Mixing and detonation structure in a rotating detonation engine with an axial air inlet, *Proceedings of the Combustion Institute* (2020).

[17] K. Ishii, M. Kojima, Behavior of detonation propagation in mixtures with concentration gradients, *Shock Waves* 17 (2007) 95–102.

[18] D. Kessler, V. N Gamezo, E. Oran, Gas-phase detonation propagation in mixture composition gradients, *Philosophical transactions of the Royal Society. Series A, Mathematical, Physical, and Engineering Sciences* 370 (2012) 567–96.

[19] D. Santavicca, R. Yetter, S. Peluso, Effect of mixture concentration inhomogeneity on detonation properties in pressure gain combustors, university turbine systems research (utsr) 2015 kick-off meeting (presentation), 2015.

[20] L. R. Boeck, F. M. Berger, J. Hasslberger, T. Sattelmayer, Detonation propagation in hydrogen–air mixtures with transverse concentration gradients, *Shock Waves* 26 (2016) 181–192.

[21] X. Mi, *et al.*, Propagation of gaseous detonation waves in a spatially inhomogeneous reactive medium, *Phys. Rev. Fluids* 2 (2017) 053201.

[22] X. Mi, E. V. Timofeev, A. J. Higgins, Effect of spatial discretization of energy on detonation wave propagation, *Journal of Fluid Mechanics* 817 (2017) 306338.

[23] S. Prakash, R. Fiévet, V. Raman, The effect of fuel stratification on the detonation wave structure, AIAA Paper 2019-1511, 2019.

[24] V. Eswaran, S. B. Pope, Direct numerical simulations of the turbulent mixing of a passive scalar, *The Physics of Fluids* 31 (1988) 506–520.

[25] M. Hassanaly, V. Raman, H. Koo, M. B. Colket, Influence of Fuel Stratification on Turbulent Flame Propagation, AIAA Paper 2015-0426, 2015.

[26] S. Boulal, P. Vidal, R. Zitoun, Experimental investigation of detonation quenching in non-uniform compositions, *Combustion and Flame* 172 (2016) 222 – 233.

[27] H. Koo, V. Raman, Large-eddy simulation of a supersonic inlet-isolator, *AIAA Journal* 50 (2012) 1596 – 1613.

[28] R. Fiévet, V. Raman, Effect of vibrational nonequilibrium on isolator shock structure, *J. of Prop. and Power* 34 (2018) 1334–1344.

[29] P. Donde, H. Koo, V. Raman, A multivariate quadrature based moment method for les based modeling of supersonic combustion, *Journal of Computational Physics* 231 (2012) 5805 – 5821.

[30] H. Koo, V. Raman, P. L. Varghese, Direct numerical simulation of supersonic combustion with thermal nonequilibrium, *Proceedings of the Combustion Institute* 35 (2015) 2145 – 2153.

[31] G. Jiang, D. Peng, Weighted eno schemes for hamilton–jacobi equations, *SIAM Journal on Scientific Computing* 21 (2000) 2126–2143.

[32] M. Herrmann, G. Blanquart, V. Raman, Flux corrected finite-volume scheme for preserving scalar boundedness in large-eddy simulations, AIAA Paper 2005-1282, 2005.

[33] M. A. Mueller, T. J. Kim, R. A. Yetter, F. L. Dryer, Flow reactor studies and kinetic modeling of the h2/o2 reaction, *International Journal of Chemical Kinetics* 31 (1999) 113–125.

[34] R. J. Kee, F. M. Rupley, J. A. Miller, Chemkin-II: A Fortran chemical kinetics package for the analysis of gas-phase chemical kinetics, Tech. Rep., United States, 1989.

[35] J. R. Burr, K. Yu, Detonation wave propagation in cross-flow of discretely spaced reactant jets, AIAA Paper 2017-4908, 2017.